Examining Scar Revival Times of Different Incident Atomic Geometries

Peiqi (Maggie) Chen, June Lee, Diya Naik, Youhao Wang

April 14, 2024

1 Introduction

Quantum scars are fascinating natural phenomena and arguably the first new discovery provided by fully implemented quantum computers. The quantum scar is at its heart a system with oscillatory non-ergodic behavior, leading it to oscillate between states determined by initial conditions. This phenomenon leads to long-time coherent dynamics in a format somewhat similar to the behavior of a damped oscillator.

To set up a quantum scar, we must first prepare a many-body quantum system. This system is then given a "kick" of energy, a process called "quenching", after which it evolves according to a fixed time-based Hamiltonian operator. While at first the system's evolution is relatively incoherent and unpredictable, the evolution eventually converges into a state profoundly similar to the initially prepared system. The many-body system continues to evolve–through this evolution it oscillates back to the initial state, and back to the evolution convergent state, back and forth until the system gradually loses coherence. The generalized Hamiltonian operator governing this kind of system can be exemplified by

$$H = \frac{\Omega(t)}{2}(|g\rangle\langle r| + |r\rangle\langle g|) - \sum_i \delta(t) n_i + \sum_{i<j} V_{ij} n_i n_j$$

where σ_x is the state flipping operator $|g\rangle\langle r| + |r\rangle\langle g|$ that transforms the ground state $|g\rangle$ to the excited Rydberg state $|r\rangle$ and vice versa.

From $H = \frac{\Omega}{2}\sigma_x$ and $|\psi(0)\rangle = |g\rangle$,

$$\psi(t) = \cos(\frac{\Omega}{2}t)\,|g\rangle - i\sin(\frac{\Omega}{2}t)\,|r\rangle$$

Another related relationship that contributes to the phenomena we are trying to perturb to find the highest scar revival is the effect of the Rabi drive on a single and multiple atoms. Rabi oscillations is a canonical phenomenon in quantum dynamics in which given a single two-level-system (qubit start in the $|0\rangle$ of the computational $\hat{z}$-basis), and a driving field around an axis not parallel with this z, we observe oscillations in the qubit state. This is important since it explains that as time t advances in the scenario where a constant field is in the direction perpendicular to z, the state of our qubit would oscillate sinusoidally between the initial state $|g\rangle$ (ground) and excited state $|r\rangle$ (Rydberg state).

2 Methods

After determining the problem at hand, our plan was to test different shapes. This would be done in simulation to compare and determine what had better state revival chances before testing on hardware, and we ended up tinkering with three main shapes: a linear chain, a square tile, and a chain closed into a cycle. We mainly implemented "detuning" to code laser tuning methods (that'll be eventually connected to hardware) to frequencies slightly offset from the resonant frequency of our system. Within the system, the laser excites atoms from ground state to a higher-energy Rydberg state. This makes them bigger, which contributes to the process of "quench." Throughout our experimentation, we faced some difficulties and went through frequent debugging. We started out spending time learning how this new code library worked. However, the code in the tutorial given to us was not working and did not result in any meaningful results. To resolve these issues, we translated the code back into pseudo-code to determine if there were flaws with our logic flow, referenced resources, experimented with various values for different variables (or, as we fondly call it: "breaking the code"). Other times, we would be running our code for longer than necessary (sometimes up to 40 minutes when it should have taken approximately 9-15 secs), and we figured out that changing the spacing of our geometric spaces can also contribute to the time efficiency of our simulation.

3 Plots

After getting a handle on the quantum scar phenomenon using the tutorial chain system, we sought out experiments that contained large amounts and small amounts of atom-atom interaction. By understanding more extreme phenomena, we would be able to think about which extrema would be better to stay away from–or whether to avoid extrema entirely.

3.0.1 Default Chain

This was the first system we experimented with. A dead simple arrangement of atoms in a line, this was the system first given to us in the tutorial. It has very few atom-atom interactions by its geometry

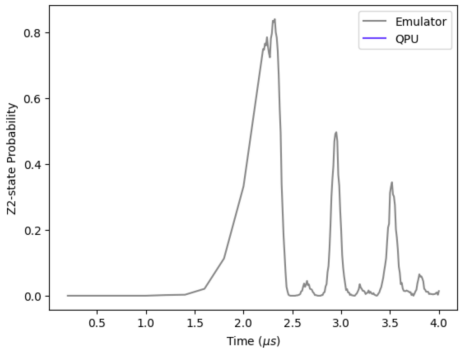

Figure 1: Probability plot over time of Bloqade tutorial's default chain

3.0.2 Square

In seeking out experimentation with large amounts of atom-atom interaction, this seemed our best bet for being able to use a reasonably low amount of computing power to be able to experiment with values while still maintaining a large number of interactions between atoms.

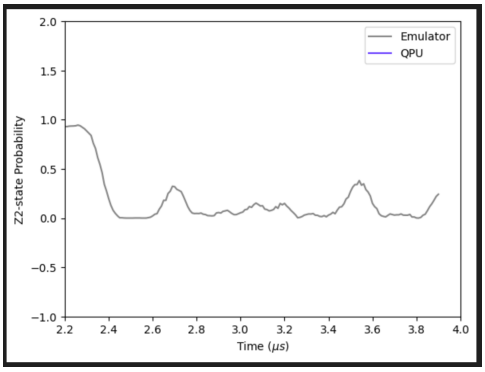

Figure 2: Probability plot over time of a 3 x 3 square lattice while applying $\delta = 42.66$ and $\Omega = 15.8$

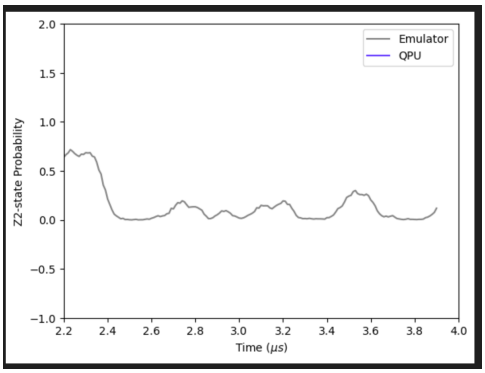

Figure 3: Probability plot over time of a 3 x 3 square lattice while applying $\delta = 42.66$ and $\Omega = 90$

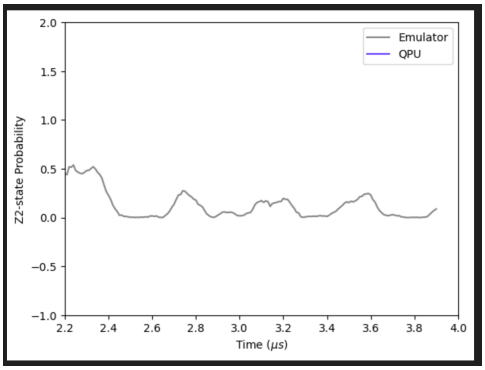

Figure 4: Probability plot over time of a 3 x 3 square lattice while applying $\delta = 42.66$ and $\Omega = 120$

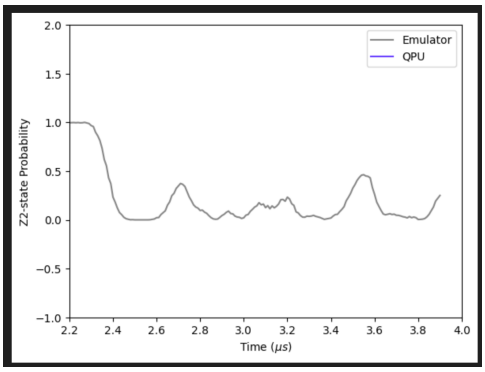

Figure 5: Probability plot over time of a 3 x 3 square lattice while applying $\delta = 42.66$ and $\Omega = 15.8$

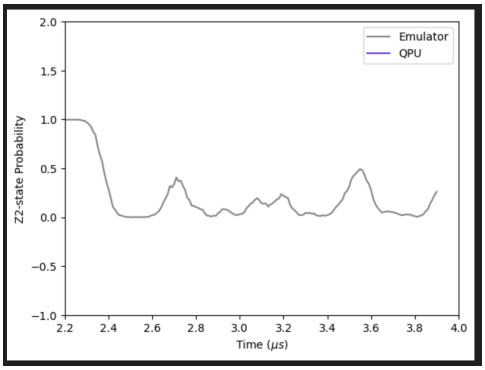

Figure 6: Probability plot over time of a 3 x 3 square lattice while applying $\delta = 80$ and $\Omega = 30$

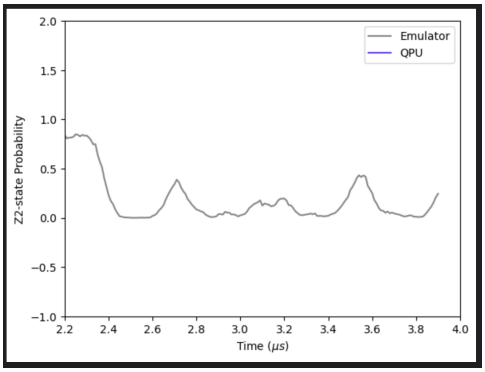

Figure 7: Probability plot over time of a 3 x 3 square lattice while applying $\delta = 80$ and $\Omega = 90$

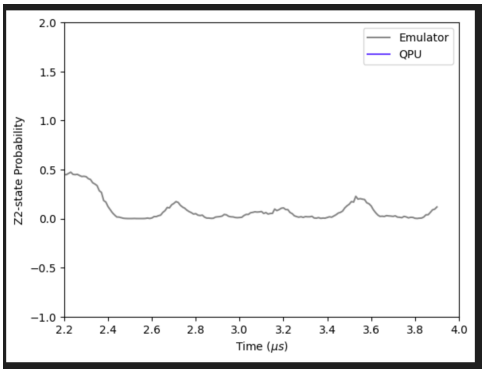

Figure 8: Probability plot over time of a 3 x 3 square lattice while applying $\delta = 120$ and $\Omega = 30$

task_number	0	1	2	3	4	5	6	7	8
0	0.00	0.00	0.00	0.00	0.00	0.00	0.00	0.00	0.00
1	0.02	0.01	0.02	0.00	0.00	0.01	0.01	0.02	0.02
2	0.02	0.00	0.03	0.02	0.04	0.00	0.03	0.06	0.03
3	0.09	0.06	0.07	0.06	0.06	0.04	0.07	0.03	0.06
4	0.10	0.06	0.12	0.08	0.10	0.11	0.07	0.05	0.08
5	0.25	0.13	0.27	0.12	0.09	0.11	0.15	0.16	0.27
6	0.44	0.17	0.42	0.18	0.11	0.13	0.42	0.18	0.44
7	0.82	0.02	0.84	0.01	0.36	0.04	0.88	0.03	0.84
8	0.82	0.04	0.87	0.06	0.63	0.03	0.80	0.04	0.85
9	0.96	0.01	0.90	0.01	0.86	0.02	0.88	0.00	0.93
10	0.97	0.01	0.97	0.01	0.93	0.01	0.97	0.01	0.95
11	0.97	0.01	0.96	0.01	0.98	0.02	0.98	0.01	0.96
12	0.22	0.04	0.27	0.03	0.55	0.02	0.31	0.07	0.28
13	0.39	0.32	0.34	0.34	0.23	0.37	0.38	0.32	0.37
14	0.47	0.09	0.39	0.11	0.47	0.12	0.37	0.11	0.32
15	0.27	0.15	0.39	0.23	0.19	0.18	0.38	0.23	0.31
16	0.38	0.30	0.35	0.31	0.33	0.25	0.32	0.33	0.35
17	0.31	0.25	0.38	0.21	0.24	0.20	0.27	0.28	0.32
18	0.53	0.13	0.57	0.13	0.56	0.15	0.53	0.16	0.50
19	0.30	0.14	0.31	0.10	0.58	0.12	0.33	0.11	0.30

Figure 9: Table of state revival probability of a 9 qubit square lattice while applying $\delta = 80.0$ and $\Omega = 30.00$

3.0.3 Augmented Cycle

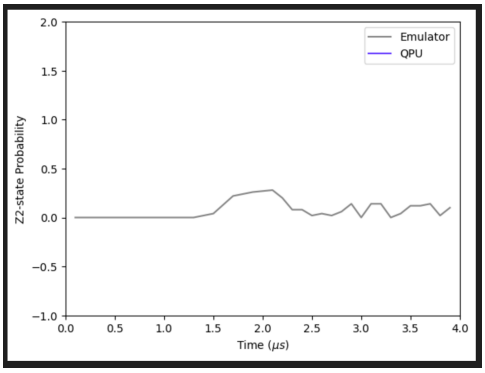

Figure 10: Probability plot over time of a 10 qubit closed chain with single-qubit augmentation while applying $\delta = 42.66$ and $\Omega = 15.8$

task_number	0	1	2	3	4	5	6	7	8	9	10
0	0.00	0.00	0.00	0.00	0.00	0.00	0.00	0.00	0.00	0.00	0.00
1	0.02	0.00	0.00	0.00	0.00	0.00	0.00	0.00	0.00	0.00	0.00
2	0.00	0.00	0.00	0.00	0.00	0.00	0.00	0.00	0.02	0.00	0.00
3	0.00	0.00	0.02	0.02	0.06	0.02	0.04	0.00	0.02	0.00	0.04
4	0.06	0.02	0.10	0.02	0.12	0.06	0.04	0.06	0.02	0.08	0.02
5	0.10	0.10	0.16	0.12	0.10	0.10	0.12	0.14	0.08	0.10	0.20
6	0.14	0.36	0.24	0.30	0.18	0.34	0.14	0.30	0.30	0.04	0.74
7	0.18	0.62	0.28	0.46	0.36	0.36	0.42	0.30	0.54	0.00	0.92
8	0.34	0.60	0.34	0.56	0.38	0.46	0.46	0.44	0.54	0.00	0.98
9	0.36	0.64	0.30	0.56	0.42	0.44	0.50	0.44	0.56	0.00	1.00
10	0.46	0.54	0.44	0.44	0.46	0.42	0.52	0.32	0.68	0.00	1.00
11	0.38	0.62	0.38	0.50	0.44	0.44	0.42	0.50	0.50	0.06	0.92
12	0.20	0.80	0.20	0.62	0.30	0.60	0.36	0.60	0.40	0.00	1.00
13	0.24	0.66	0.22	0.46	0.22	0.34	0.38	0.28	0.54	0.04	0.76
14	0.38	0.10	0.44	0.18	0.34	0.18	0.20	0.30	0.36	0.12	0.36
15	0.56	0.10	0.54	0.24	0.42	0.32	0.44	0.26	0.42	0.12	0.38
16	0.60	0.10	0.24	0.20	0.28	0.28	0.26	0.26	0.48	0.06	0.58
17	0.44	0.26	0.32	0.32	0.32	0.44	0.20	0.36	0.50	0.06	0.58
18	0.40	0.36	0.38	0.30	0.28	0.32	0.36	0.22	0.44	0.04	0.50
19	0.34	0.20	0.40	0.16	0.38	0.24	0.32	0.32	0.32	0.14	0.60
20	0.40	0.28	0.46	0.22	0.40	0.26	0.44	0.20	0.54	0.14	0.56

Figure 11: Table of state revival probability of a 10 qubit closed chain with single-qubit augmentation while applying $\delta = 42.66$ and $\Omega = 15.8$

4 Discussion

After applying different Ω and δ using Bloquade's Emulator, we were able to test the fidelity of different geometries. From our plots, we determined that the probability plot of a 3x3 square matrix of qubits at $\delta = 42.66$ and $\Omega = 90$. Notably, our graphs' system of recoherence is dependent on these values that affect intial state of coherence, recoherence power, and system geometry-which is arguably more significant than the aforementioned values.

Further experiments might consider incident atomic geometries of honeycombs, Kagome matrices, and Lieb matrices. Honeycombs have been found to perform better that square matrices in neutral atom experiments, so testing different types of honeycombs would be fruitful. Specifically, decorated honeycombs have been found to do better than squares. Similarly, the augmented circle performed poorly in our simulation. There may yet be some impact of openness in system geometry found to affect re-coherence power.

5 Conclusion

Quantum scarring is unique not only for the recency of its discovery but also as a fascinating route of exploration. Particularly exciting is the ability of scarring to enable recapitulation of system coherence even after decoherence, something not often found in physical systems and phenomena. Unfortunately, due to the many-body nature of current studies of this phenomenon, mathematical analysis of the equations governing system evolution are often unable to function, leaving studies of quantum scarring to conduct experimentation to learn more about the scarring phenomenon. We found that changes in Ω and δ, which controlled quenching power and detuning, controlled the curve at recapitulation power and system stability upon initialization, respectively, and were able to make use of these observations to work towards optimizing the quantum scarring phenomenon across a simulated system of nine qubits in square lattice.

References

[1] S. Bernien, H., Schwartz, S., Keesling, A. et al. Probing many-body dynamics on a 51-atom quantum simulator. Nature 551, 579–584 (2017). https://doi.org/10.1038/nature24622

[2] S. D. Bluvstein et al. ,Controlling quantum many-body dynamics in driven Rydberg atom arrays.Science371,1355-1359(2021).DOI:10.1126/science.abg2530

[3] S. Bravyi, S., et al. "Mitigating measurement errors in multiqubit experiments," in Physical Review A, vol. 103, no. 4, 2021.

[4] S. Turner, C., et al. "Weak ergodicity breaking from quantum many-body scars," in Nature Physics, vol. 14, no. 7, pp. 745–749, 2018.